

# PCCP

Accepted Manuscript



This is an *Accepted Manuscript*, which has been through the Royal Society of Chemistry peer review process and has been accepted for publication.

*Accepted Manuscripts* are published online shortly after acceptance, before technical editing, formatting and proof reading. Using this free service, authors can make their results available to the community, in citable form, before we publish the edited article. We will replace this *Accepted Manuscript* with the edited and formatted *Advance Article* as soon as it is available.

You can find more information about *Accepted Manuscripts* in the [Information for Authors](#).

Please note that technical editing may introduce minor changes to the text and/or graphics, which may alter content. The journal's standard [Terms & Conditions](#) and the [Ethical guidelines](#) still apply. In no event shall the Royal Society of Chemistry be held responsible for any errors or omissions in this *Accepted Manuscript* or any consequences arising from the use of any information it contains.

## Interactions of ionic liquids with hydration layer of poly(N-isopropylacrylamide): Comprehensive analysis of biophysical techniques results

P. Madhusudhana Reddy, R. Umapathi and P. Venkatesu\*

Department of Chemistry, University of Delhi, Delhi-110 007, India

\*Author to whom correspondence should be addressed; E-mail: venkatesup@hotmail.com; venkatesu@chemistry.du.ac.in (P. Venkatesu)

### Abstract

Here, we report comprehensive analysis of biophysical techniques results for the influence of ionic liquids (ILs) containing same cation, 1-Butyl-3-methylimidazolium ( $\text{Bmim}^+$ ) and commonly used anions such as  $\text{SCN}^-$ ,  $\text{BF}_4^-$ ,  $\text{I}^-$ ,  $\text{Br}^-$ ,  $\text{Cl}^-$ ,  $\text{CH}_3\text{COO}^-$  and  $\text{HSO}_4^-$  on phase transition temperature of poly(N-isopropylacrylamide) (PNIPAM) aqueous solution. Further, the effect of these ILs on bovine serum albumin (BSA) has also been studied. The modulations in UV-visible (UV-vis) absorption spectra, fluorescence intensity spectra, viscosity ( $\eta$ ), hydrodynamic diameter ( $d_H$ ) fourier transform infrared (FTIR) spectra and scanning electron microscopy (SEM) micrographs clearly reflect the change in hydration state of PNIPAM in the presence of ILs. The observed single phase transition of PNIPAM aqueous solution at higher concentration of IL is the result of weak ion-ion pair interactions in IL.

## Introduction

Amphiphilic polymers have been studied as potential materials due to their both theoretical and practical applications in many research fields such as drug delivery, pharmaceutical, membranes, agriculture, and personal care products.<sup>1-6</sup> Poly(N-isopropylacrylamide) (PNIPAM) is the most widely studied thermoresponsive polymer, which shows a lower critical solution temperature (LCST) of  $\sim 33$  °C in water.<sup>7,8</sup> Below the LCST, PNIPAM is hydrated and adopt an extended coil conformation.<sup>9</sup> PNIPAM aqueous solution undergoes a sharp and reversible coil-to-globule transition upon heating.<sup>10</sup> The main rationale in the selection of PNIPAM for the present study is not only due to its LCST that is close to body temperature but also due to its unique sensitivity to environmental conditions such as pH,<sup>11</sup> ionic strength,<sup>12</sup> pressure etc.<sup>13</sup> This behavior has attracted considerable attention from various scientific communities.<sup>14-17</sup>

Several studies have been attempted to explore the behavior of phase transition temperature of PNIPAM in the presence of various additives including salts,<sup>18,19</sup> surfactants,<sup>20-22</sup> co-solvents,<sup>23-25</sup> urea,<sup>26</sup> sugars,<sup>27</sup> ionic liquid<sup>7</sup> and osmolytes.<sup>8,9</sup> From these results one can draw the conclusion that, the effect of each additive on LCST of PNIPAM is unique. For instance, urea depress the LCST of PNIPAM through direct binding to the polymer molecules wherein it acts as a cross linker between PNIPAM molecules.<sup>19</sup> Whereas, trimethylamine N-oxide (TMAO) decreases LCST value by forming hydrogen bonds with water molecules that are surrounded the amide group of polymer.<sup>8</sup> Further, studies deal with the effect of anions and cations of ionic salts on phase transition of macromolecules lead to various conclusions. For instance, Cremer et al.,<sup>12,19</sup> reported that the dehydration of PNIPAM is resulted exclusively from anions. However, Du et al.<sup>28</sup> revealed through computational study that the interactions between cations and the oxygen atom of the carbonyl group of PNIPAM is the paradigm for the phase transition of PNIPAM. In another study, Algaer and van der Vegt<sup>29</sup> and Rembert et al.<sup>30</sup> revealed through MD simulations that anions of ionic salts bind stronger than that of cations. Further, they have also revealed that the binding is mainly depending upon nature of the nonpolar/polar binding sites of macromolecule. Hence, the binding is site specific. In this context, it is very important to have the complete knowledge of individual additive effect on LCST of PNIPAM to avoid unwanted results while using the additives to control the LCST of PNIPAM.

In view of importance of additives in controlling the phase transition of polymers, ILs have been proved as potential additives<sup>7</sup> and solvents to control the phase transition

temperatures of polymer.<sup>31,32</sup> Further, ILs are useful in many fields of chemistry, material science and industry.<sup>33,34</sup> In the light of growing importance of ILs, researchers are actively using ILs in protein science.<sup>35-37</sup> Indeed, ILs are extended their hands of applications not only into the protein science but also into the critical mixtures of binary solvents.<sup>38,39</sup>

Hence, the main aim of the present study is to shed the more light on the topic of effect of various ILs on the phase transition temperature of PNIPAM aqueous solution. For this purpose, in the present study we have investigated the effect of series of ILs containing the same cation, 1-butyl-3-methylimidazolium ( $\text{Bmim}^+$ ) and commonly used anions such as chloride ( $\text{Cl}^-$ ), bromide ( $\text{Br}^-$ ), hydrogen sulfate ( $\text{HSO}_4^-$ ), tetrafluoroborate ( $\text{BF}_4^-$ ), thiocyanate ( $\text{SCN}^-$ ), iodide ( $\text{I}^-$ ) and acetate ( $\text{CH}_3\text{COO}^-$ ). UV-visible spectroscopy (UV-vis), fluorescence spectroscopy, viscosity ( $\eta$ ), dynamic light scattering (DLS), Fourier transform infrared (FTIR) spectroscopy and scanning electron microscope (SEM) were employed to monitor the changes in hydration state of PNIPAM in the presence of ILs. To our knowledge, this is the first direct measurement to explore the ionic strength of anions of ILs on LCST of PNIPAM. Further, the present work may make an easy path in selection of ILs for the tailoring of thermoresponsive behaviour of amphiphilic polymers.

Additionally, we have also described the effect of these ILs on a protein, bovine serum albumin (BSA). BSA is a type of popular protein model because of its many applications, both in clinical medicine and in basic research and thereby we chose it as a protein model in the present study. BSA is also known to bind variety of biologic probe molecules. BSA is a single polypeptide chain of molecular weight of 66 kDa consisting of 583 amino acid residues. In folding and unfolding of BSA, mainly 17 disulphide bridges take prominent role. Albumin is the most abundant soluble protein in the body of all vertebrates and is the most plasma protein in the blood.<sup>40</sup>

## Materials and Methods

### Materials and Sample Preparation

PNIPAM ( $M_n = 20000-25000$ ), BSA (66 kDa), 1-butyl-3-methylimidazolium thiocyanate (0.7% water), 1-butyl-3-methylimidazolium hydrogensulfate ( $\leq 1.0\%$  water), 1-butyl-3-methylimidazolium tetrafluoroborate ( $\leq 0.05\%$  water), 1-butyl-3-methylimidazolium chloride ( $\leq 0.2\%$  water), 1-butyl-3-methylimidazolium bromide ( $\leq 200$  ppm water), 1-butyl-3-methylimidazolium iodide ( $\leq 0.5\%$  water) and 1-butyl-3-methylimidazolium acetate ( $\leq 0.5\%$

water) were provided by the Sigma-Aldrich chemical co. (USA). The chemical structure of PNIPAM has displayed in Fig. 1.

All sample solutions were prepared by dissolving an appropriate amount of polymer and ILs into purified water produced by a NANO pure ultrapure water system (Rions India, India) and had a minimum resistivity of 18.3 M $\Omega$  cm. Except in Fourier transform infrared (FTIR) spectroscopy, the concentration of PNIPAM was maintained at 6 mg/mL in all studies. For FTIR spectroscopy studies samples were prepared with 15 mg/mL of PNIPAM. Each IL effect on LCST of PNIPAM studied under three concentrations (5, 10 and 15 mg/mL). The concentration of BSA was 20 mg/mL. All resulting sample solutions were incubated for 24 h at room temperature. Before performing the measurements, the sample solutions were filtered with 0.45  $\mu$ m disposable filters (Millipore, Millex-GS) through a syringe to remove the dust particles if any present. 8-anilino-1-naphthalenesulfonic acid (ANS) ( $2 \times 10^{-5}$  M) was used as an external probe in UV and fluorescence measurements.

#### **Uv-vis Absorption Measurements**

Ultraviolet-visible (UV-Vis) absorption spectra of the PNIPAM and BSA were recorded from 190 to 800 nm by means of a double beam UV-visible spectrophotometer (UV-1800, Shimadzu Co., Japan) at room temperature. An aliquot of sample solution was transferred uniformly in to the quartz cell of 1 cm path length. Spectrophotometer has matched quartz cells, with spectral bandwidth of 1 nm, wavelength accuracy of  $\pm 0.3$  nm with automatic wavelength corrections.

#### **Fluorescence Intensity Measurements**

Fluorescence spectra were acquired by using a Cary Eclipse fluorescence spectrophotometer (Varian optical spectroscopy instruments, Mulgrave, Victoria, Australia) with an intense Xenon flash lamp as the light source. This instrument was equipped with multicell holder, which was electro-thermally controlled at precise temperature regulated by peltiers. The temperature control of the peltier thermostatted cell holders is extremely stable over time, with precision of  $\pm 0.05$   $^{\circ}$ C. The emission spectra were recorded with a slit width of 2.5/2.5 nm and a PMT voltage of 720 V. The scan speed was kept at 1200 nm min $^{-1}$ . Temperature-dependent spectra were collected between 25-45  $^{\circ}$ C in intervals of 1  $^{\circ}$ C, with an accuracy of  $\pm 0.1$   $^{\circ}$ C. For temperature-dependent measurements, the samples were equilibrated for at least 20 min at each temperature before measurement.

#### **Viscosity Measurements**

Viscosity ( $\eta$ ) measurements were continuously measured using a commercial sine-wave vibro viscometer (SV-10 A&D Company Limited, Japan), with a normal uncertainty of  $\pm 0.01$  mPa.s. This instrument provides the measurements by detecting the driving electric current necessary to resonate the two sensor plates at a constant frequency of 30 Hz and amplitude of less than 1 mm. Temperature was controlled at any chosen temperature with a precision of  $\pm 0.2$  °C by means of thermostatically controlled, well-stirred circulated water bath (LAUDA alpha 6, Japan) with digital temperature display. All  $\eta$  measurements of the sample were collected at heating rate of 1 °C/20 min after allowing the sample to attain thermodynamic equilibrium. The measurement chamber of the viscometer is closed during the collection of  $\eta$  measurements in order to avoid the loss of water by evaporation.

#### **Dynamic Light Scattering (DLS) Measurements**

Dynamic light scattering (DLS) measurements were performed on a Zetasizer Nano ZS90 (Malvern Instruments Ltd., UK) at a scattering angle of 90° and analyzed by Malvern Zetasizer Software version 6.01. The instrument was provided with 4 mW He-Ne laser with a fixed wavelength,  $\lambda = 633$  nm as a light source and utilized to characterize the obtained aggregate sizes. All of the DLS experiments were performed as a function of temperature in thermostatic sample chamber which was maintained at desired temperatures within a temperature range of 2–90 °C. Temperature of the measurements was controlled with an accuracy of  $\pm 0.1$  °C. A filtered bubble free sample of around 1.5 mL was transferred into quartz sample cell which was sealed with a Teflon-coated screw cap to secure from dust. Then the airtight sample was introduced into the sample holder of sample chamber of DLS instrument. The Brownian motion of particles was detected by DLS and it was correlated to the particle size. The hydrodynamic radii ( $d_H$ ) of aggregates can be extracted through the following Stokes-Einstein equation.

$$d_H = \frac{kT}{3\pi\eta D} \quad (1)$$

where  $k$  is the Boltzmann's constant ( $1.3806503 \times 10^{-23}$  m<sup>2</sup> kg s<sup>-2</sup> K<sup>-1</sup>),  $T$  is absolute temperature (K),  $\eta$  is viscosity (mPa.s), and  $D$  is diffusion coefficient (m<sup>2</sup> s<sup>-1</sup>). All data were obtained from the instrumental software.

#### **Fourier transform infrared (FTIR) spectroscopy**

The infrared spectrum was recorded on a iS 50 FT-IR (ThermoFisher scientific) spectrometer. The PNIPAM sample dissolved in water or aqueous IL solutions was put into an IR cell with two ZnSe windows. A Chromel-Alumel K-type thermocouple is provided for

continuous monitoring of the temperature on the inside of the sample chamber. Each IR spectrum reported here was an average of 200 scans using a spectral resolution of  $4\text{ cm}^{-1}$ . The IR spectra were recorded and stored by using spectroscopic software (Varian Resolutions, Version 4.10). A background spectrum was obtained directly before sample spectra. Specifically, for each sample containing PNIPAM, an otherwise identical IL solution without the polymer was used as background.

### SEM Measurements

SEM studies were carried out using Carl Zeiss EVO 40 electron microscope operating at 20 kV. Samples were mounted on a double-sided adhesive carbon disk and sputter-coated with a thin layer of gold to prevent sample charging problems.

### Results

Changes in the absorption and emission bands of UV-vis and fluorescence spectra indicate changes in the environment of ANS contributed from the change in hydration states of PNIPAM. ANS exhibits two characteristic absorption peaks at the  $\lambda_{\text{max}} \sim 370$  or  $270\text{ nm}$ .<sup>41</sup> However, in the present experiment we have considered the changes in the peak at  $\lambda_{\text{max}} 360\text{ nm}$  as this peak is sensitive for changes in its microenvironment. As shown in Fig. 2, the absorption of ANS in polymer aqueous solution is minimum in the absence of ILs. This feature is resulted from the well hydrated coil conformation of PNIPAM shows less affinity for hydrophobic probes such as ANS.<sup>42</sup> However, by the addition of IL to the polymer aqueous solution the absorption of the ANS enhanced accompanying with bathochromic shift in wavelength of absorption maxima, which suggests that the hydrophobic collapse of the polymer. Further, the process of hydrophobic collapse of polymer is more pronounced at the higher concentration of IL (Figs. S1 and S2 in supplementary material). However, the pattern of spectra in all the three concentrations was same. It should be noted from studied UV-Vis spectra (Fig. 2) that the  $\text{HSO}_4^-$  ion has the maximum ability to perturb the hydration layer around the polymer molecule which ultimately leads to the enhancement of hydrophobic collapse process of polymer in the solution. The present UV-visible results are strongly consistent with the results of absorption studies of ANS and pyrene, over the gemini surfactant aqueous solution.<sup>43,44</sup>

Fig. 3 delineates the fluorescence spectra of ANS in PNIPAM aqueous solution in the absence and presence of ILs ( $5\text{ mg/mL}$ ) at  $25\text{ }^\circ\text{C}$ . The Fig. 3 reveals that ANS exhibits low intensity in water at wavelength of  $510\text{ nm}$  and even the intensity enhancement is not significant in the PNIPAM aqueous solution. However, the ANS emission intensity is

increased and eventually reached a maximum with the addition of IL. This indicates that IL plays a significant role in inducing nanoscale aggregation of PNIPAM in aqueous medium. Further, this enhancement is more pronounced in the case of ILs containing kosmotropic anion than that of ILs containing chaotropic anion. It is interesting to note that the fluorescence intensity is considerably maximum in the case of IL containing  $\text{HSO}_4^-$  among the studied anions. The intensity is increased with increasing the concentration of IL which is a direct result for the increasing hydrophobic collapse of PNIPAM in the higher concentration of ILs (Figs. S3 and S4 in supplementary material).

The temperature dependence fluorescence intensity of ANS in PNIPAM aqueous solution in the presence and absence of ILs (5 mg/mL) has been shown in Fig. 4. The temperature-dependent intensity profiles for the concentrations of 10 and 15 mg/mL in the temperature range of 25-45 °C have been given in supplementary material (Figs. S5 and S6). As expected, in the PNIPAM aqueous solution, ANS exhibits drastic enhancement in intensity at LCST value (33 °C). Interestingly, the intensity was found to increase sharply in all studied samples in the presence of ILs even at low temperatures. It is evident that all investigated ILs depress the cloud-point curves to different extents depending upon their position in the Hofmeister sequence, with the  $\text{HSO}_4^-$  ion being the most effective.

Although there are number of techniques available to monitor the coil-globule transition of PNIPAM under various stimuli,  $\eta$  measurements stand as a technique of choice.<sup>7,8,45,46</sup> In Fig. 5,  $\eta$  values for PNIPAM aqueous solution with and without ILs are plotted as a function of temperature. As one might expect, below the polymer's LCST, the solution has a larger  $\eta$  values due to the hydrated coil conformation. On the other hand, above its LCST, the polymer becomes dehydrated and it would collapse and takes to the compact globule structure; therefore, the solution has a lower  $\eta$ .<sup>7,8,45,46</sup> Indeed, the LCST is lowered by the addition of the IL. However, IL containing  $\text{HSO}_4^-$  is the one among the others that exerts strong effect on LCST values. We have observed similar trend for remaining two concentrations (Figs. S7 and S8) with further diminishment in  $\eta$  values.

The hydrodynamic diameter ( $d_H$ ) of the aggregates is known as finger print for detecting the hydrophobic collapse of PNIPAM in aqueous medium.<sup>47</sup> The  $d_H$  values of PNIPAM aggregates in aqueous solution without and with ILs (5 mg/mL) were plotted in Fig. 6 as a function of temperature. It is clearly seen from this figure that there is no noticeable change in  $d_H$  till 33 °C, however, dramatic increase in the  $d_H$  value was observed for PNIPAM aqueous solution at 33 °C that reflects the enhancement of the collapsed state



and this point is called as LCST. In contrast to this, PNIPAM shows phase transition even at lower temperature in the presence of various ILs. As shown in Fig. 6,  $\text{HSO}_4^-$  shows maximum ability to induce the hydrophobic collapse of PNIPAM, whereas  $\text{SCN}^-$  shows minimum ability to induce the hydrophobic collapse of PNIPAM and remaining ions lie in between these two ions. Specifically, the degree of diminishment of LCST by anions is more pronounced at higher concentrations of 10 and 15 mg/mL (Figs. S9 and S10) and it is obvious. The same behaviour was observed previously for PNIPAM in aqueous solutions of soluting-out agents such as IL,<sup>7</sup> osmolyte,<sup>8</sup> salts<sup>12</sup> and buffers.<sup>47</sup>

To obtain the dehydration mechanism of PNIPAM in the presence of various ILs, we further studied, FTIR spectroscopy analysis for all the sample solutions. In the present study, frequencies of the amide I and II bands is mainly considered to understand the dehydration mechanism of PNIPAM. The amide I peak is mainly due to C=O stretching vibrations, whereas the amide II peak consists of a combination of N-H bending with C-H stretching vibrations. The amide I and II peaks provide valuable information regarding hydrogen bonding of the amide group. Fig. 7, shows the variations in amide band I and II in the presence of different ILs at 25 °C. As shown in the figure, the amide I and II bands of PNIPAM in pure water below the LCST appear at 1623 and 1560  $\text{cm}^{-1}$ , respectively. The single peak of amide I band at 1623  $\text{cm}^{-1}$  indicates that all the carbonyl groups are hydrogen bonded to water.<sup>48</sup> Based on experimental and theoretical studies,<sup>48</sup> the C=O group is considered to be hydrogen-bonded to two water molecules, and the N-H group forms a hydrogen bond with an oxygen atom of water. Maeda *et al.*<sup>49</sup> have observed that the amide I band of PNIPAM could be fitted with a single Gaussian component below the LCST (1625  $\text{cm}^{-1}$ ) and with two components (1625  $\text{cm}^{-1}$  and 1650  $\text{cm}^{-1}$ ) above the LCST. In our present study also, the new peak has been observed ~1648 by the addition of IL and which indicated that dehydration of PNIPAM by forming inter and intra molecular hydrogen bonding between carbonyl and amine functional group of polymer. Moreover, the intensity of this peak is further enhanced with increasing the concentration of ILs (Figs. S11 and S12).

To address comprehensive picture for influence of counter ion on coil-globule transition of PNIPAM, SEM micrographs were also collected for the samples of PNIPAM aqueous solution in the presence of IL containing  $\text{HSO}_4^-$  (strongest inducer for hydrophobic collapse of PNIPAM) and  $\text{SCN}^-$  (weakest inducer of hydrophobic collapse of PNIPAM) at room temperature and displayed in Fig. 8. The SEM micrograph (Fig. 8a) of PNIPAM aqueous solution without IL, clearly exemplifies coiled structure of PNIPAM. However, in

the presence of  $\text{SCN}^-$  hydrogen bonds between the polymer and water molecules are ruptured by the anions of IL, thereby, the polymer underwent hydrophobic collapse and ultimately contributing to the nano scale range aggregation of PNIPAM molecules (Fig. 8b). On the other hand, kosmotropic anion,  $\text{HSO}_4^-$  enhances more hydrophobic collapse of PNIPAM by rupturing hydrogen bonds and leads to the more compact structure of PNIPAM (Fig. 8c). However, the hydrophobic collapse of PNIPAM molecules more pronounced at higher concentration (15 mg/mL) of ILs as shown in the Fig. 8d and 8e for  $\text{SCN}^-$  and  $\text{HSO}_4^-$ , respectively.

For the sake of clarity and presentation into the role of concentration of IL ([Bmim][ $\text{HSO}_4$ ]) on hydrophobic collapse of polymer, we have depicted the all experimental results in Fig. 9 as a function of IL concentration. As shown in Fig. 9b, the wavelength was shifted from 516 nm (in the absence of IL) to 494, 491 and 482 in the presence of 5, 10 and 15 mg/mL of IL, respectively. Further, the FTIR results in Fig. 9f reveals, pure PNIPAM aqueous solution does not show any peak at  $1648\text{ cm}^{-1}$  and which can be attributed from the absence of inter and intra molecular hydrogen bonds among polymer chains. However, with the addition of IL, the new peak has been observed at  $1648\text{ cm}^{-1}$  and this can be a characteristic for inter and intra chain hydrogen bond between carbonyl group and amine group of polymer. Moreover, the intensity of the peak at  $1648\text{ cm}^{-1}$  is further increased with the enhancement of IL concentration. From the enhancement in intensity of peak at  $1648\text{ cm}^{-1}$  one can clearly understand that the concentration of IL plays significant role in promoting the polymer towards dehydrated state. As shown in Fig. 9, the modulations in each technique results can be seen by increasing the concentration of IL. However, for the sake of clarity, we have not provided other IL concentrations effect on PNIPAM aqueous solution with various techniques, since we observed the similar trend for other ILs.

Eventually, to validate our experimental results of PNIPAM, we have checked the anion tendency in protecting the folded conformation of BSA, at  $25\text{ }^\circ\text{C}$ . BSA protein has homologous tryptophan (Trp), at position 212, plus a second one at position 134. Apart from this, BSA consists of 20 tyrosine (Tyr) residues and 27 phenylalanine (Phy-A) residues. The UV-vis absorbance spectra of BSA, between 200 and 350 nm, in various anions of IL with same cation illustrated in Fig. 10, at the concentration of 5mg/mL. As depicted in this figure, the UV absorption spectra of BSA in the absence of IL at the wavelength of 279 nm, which is a characteristic feature of Trp. Red shift in absorption maximum of tryptophan residues upon addition of ILs indicate that changes in its microenvironment are contributing from the

enhancement of hydrophobicity. It is obvious that the extent of shift in absorption maxima is maximum in the case of  $\text{HSO}_4^-$  anion, whereas minimum in the case of  $\text{SCN}^-$ , among studied anions. The degree of extent of change in Trp microenvironment polarity can be controlled by the concentration of IL. As can be seen from Figs. S13 and S14, the degree of shift in absorption maxima is relatively large in the concentrations of 10 and 15 mg/mL, respectively, than that of concentration of 5 mg/mL.

### Discussion

We have taken ANS absorption spectra (Fig. 2) into account to dictate the effect of anions of IL on LCST of PNIPAM aqueous solution. At room temperature, i.e., well below the LCST value, ANS does not exhibit any characteristic peak in the PNIPAM aqueous solution. Whereas, in the presence of IL having  $\text{SCN}^-$ , ANS exhibits characteristic peak at wavelength of  $\sim 380$  nm in PNIPAM aqueous solution. It is especially worth noting that the anions of IL significantly affected the polarity of ANS environment by rupturing the hydrogen bonded cage which is responsible for the polymer dissolution and thereby, ANS provoked shift into hydrophobic environment. Further, the characteristic peak at  $\sim 380$  nm shifted towards higher wavelength of  $\sim 408$  nm in the presence of  $\text{HSO}_4^-$  anion as shown in the Fig. 2. This indicates that  $\text{HSO}_4^-$  anion is substantially strong enough for rupturing the hydrogen bonds between polymer and water molecules, than that of  $\text{SCN}^-$  anion. However, the characteristic peak of 380 nm in the presence of  $\text{SCN}^-$  at 5 mg/mL further shifted to higher wavelengths of  $\sim 384$  and  $\sim 387$  nm in the presence of higher concentrations of 10 and 15 mg/mL, respectively as shown in the Figs. S1 and S2. These results explicitly reveal that at higher concentration of IL, the total number of anions is relatively high and because of this the degree of destabilization of soluble PNIPAM is more. Moreover, this effect is more pronounced in the case of kosmotropes.

Fig. 3 explicitly uncovers the effect of ILs on emission spectra of ANS in PNIPAM aqueous solution. It is evident from Fig. 3 that the emission spectrum (navy colour line) of ANS comprises of very weak intensity at 510 nm. Moreover, the intensity enhancement is insignificant even in PNIPAM aqueous solution, implying that negligible partitioning of ANS onto PNIPAM surface. The negligible partitioning of ANS is contributing from the cooperative hydration of PNIPAM by water molecules in aqueous solution. Whereas, with the addition of IL having  $\text{SCN}^-$  to the PNIPAM solution there is a marked gain in intensity with blue shift in emission wavelength, which implies that IL is enable to enhance the hydrophobic collapse of polymer. However, the emission wavelength of ANS shifts from 510

nm to 496 nm in the presence of IL having  $\text{HSO}_4^-$ . With further enhancement of concentration of IL, the emission spectra shifted more towards lower wavelength. For instance, emission spectra shifted from 496 nm at 5 mg/mL to 487, 475 nm at 10 and 15 mg/mL concentrations of IL, respectively (Figs. S3 and S4). It has been suggested that the bathochromic shift in the emission wavelength is due to the low mobility of probe molecules. The similar type of enhancement in intensity with the blue shift was observed during PNIPAM hydrophobic collapse process over the addition of biological surfactant, sodium cholate.<sup>50,51</sup>

Fig. 4 depicts the temperature dependence of fluorescence measurements of ANS in the PNIPAM aqueous solution under the influence of different ILs. As demonstrated in Fig. 4, in pure PNIPAM aqueous solution the intensity values increase with increasing temperature. However, the increment in intensity is not significant till solution's LCST (33 °C), thereafter sharp enhancement occur in the intensity. As there is no significant change in intensity of ANS in PNIPAM aqueous solution till LCST, it implies that PNIPAM remain in well hydrated structure and thereby ANS molecules suffer for hydrophobic surface to bind. However, the sharp enhancement in intensity at LCST is resulted from the coupling of ANS molecules onto the surface of hydrophobic portion of PNIPAM. In pure PNIPAM aqueous solution the hydrophobic collapse process is induced by thermal effect, solely. Interestingly, the intensity enhancement shifts towards lower temperature, from 32.8 to 31 °C, upon addition of different ILs having from chaotropic anion,  $\text{SCN}^-$  to kosmotropic anion,  $\text{HSO}_4^-$ , respectively at the concentration of 5 mg/mL.

The shift of higher intensities towards lower temperatures indicates that the aggregation of PNIPAM in the presence of IL is encouraged. The enhanced surface of hydrophobicity would induce partitioning of the ANS molecules to the hydrophilic-hydrophobic interfaces, where they would experience reduced mobility. Although the different anions of IL at every concentration reveal the same qualitative behaviour, important quantitative differences arise when they are compared. For instance, the LCST of PNIPAM is 31 °C at the concentration of 5 mg/mL  $\text{HSO}_4^-$ , whereas, the LCST is 29.7 °C at the concentration of 15 mg/mL  $\text{HSO}_4^-$ . To prove that the intensity enhancement is due to the polymer aggregation but not due to the interaction of IL and probe, we have performed the temperature dependent fluorescence spectroscopy for IL containing aqueous solution in the temperature range of 25-45 °C (Fig. S15). However, in this spectrum no significant change is observed as in the case of polymer aqueous solution.

The  $\eta$  value for the IL free PNIPAM aqueous solution at 25 °C is 1.43 mPa.s (Fig. 5). However, this  $\eta$  value gradually decreases to 1.42, 1.41, 1.40, 1.38, 1.37, 1.34 and 1.30 mPa.s for  $\text{SCN}^-$ ,  $\text{BF}_4^-$ ,  $\text{I}^-$ ,  $\text{Br}^-$ ,  $\text{Cl}^-$ ,  $\text{CH}_3\text{COO}^-$  and  $\text{HSO}_4^-$ , respectively at the concentration of 5 mg/mL of IL in PNIPAM aqueous solution. The diminishment in  $\eta$  value clearly revealed that the IL presumably exerts its effect on the destruction of hydrogen bonds between polymer and water molecules and tends to lead hydrophobic collapse of PNIPAM. As the  $\text{SCN}^-$  containing PNIPAM aqueous solution possess highest value of  $\eta$  (1.42 mPa.s), implies that it has a little tendency in rupturing the hydrogen bonds, whereas,  $\text{HSO}_4^-$  containing PNIPAM aqueous solution possess lowest value of  $\eta$  (1.30 mPa. s) implying that it has a great ability to rupture the hydrogen bonds and thereby, it diminishes the  $\eta$  values to larger extent. The extent of diminishment in  $\eta$ , increases with increasing the concentration of IL. These results have been shown in supplementary material (Figs. S7 and S8).

As depicted in the Fig. 6,  $d_H$  values are relatively low below the LCST, whereas significantly large after the LCST in every sample of solution. The results in Fig. 6 explicitly elucidates that the LCST region of PNIPAM aqueous solution get altered in the presence of IL at the concentration of 5 mg/mL. Obviously the  $d_H$  values of PNIPAM progressively increased from 20.6 nm in pure water at 25 °C to 21.2, 22.0, 22.9, 23.7, 24.8, 29.1 and 32.1 in the presence of  $\text{SCN}^-$ ,  $\text{BF}_4^-$ ,  $\text{I}^-$ ,  $\text{Br}^-$ ,  $\text{Cl}^-$ ,  $\text{CH}_3\text{COO}^-$  and  $\text{HSO}_4^-$ , respectively. This indicates that the process of breaking of hydrogen bonds between the amide group of the polymer and water molecules is significantly triggered by the counter ions (anions) of IL. Moreover, the LCST values of PNIPAM solution decreases with increasing the concentration of ILs (Figs. S9 and S10).

From a close inspection of Fig. 7, one can find that the amide I and II bands at 1623 and 1560  $\text{cm}^{-1}$  in water. However, by the addition of IL into the polymer aqueous solution, the new peak was observed at  $\sim 1648 \text{ cm}^{-1}$  which was attributed from the transformation of the hydrated polymer to partially hydrated by making an intra- and inter chain cross-linking between C=O and H-N groups of polymer. The peak at  $\sim 1648$  is the characteristic of an intra- and inter chain cross-linking. Further, the intensity of peak at  $\sim 1648$  is progressively increases from  $\text{SCN}^-$  to  $\text{HSO}_4^-$ . The maximum intensity was observed in the case of  $\text{HSO}_4^-$  and minimum intensity was observed in the case of  $\text{SCN}^-$ . This difference in intensity dictates that  $\text{SCN}^-$  is less effective and  $\text{HSO}_4^-$  is more effective in promoting the PNIPAM towards dehydration state. Moreover, the intensity enhancement is more pronounce with

increasing the concentration of these ILs (Figs. S11 and S12 in supplementary material) Since, these measurements were made below the phase transition temperature, one can understand that the PNIPAM is undergoing phase transition in the presence of these ILs and thereby phase separation exhibits at low temperatures.

Finally, by taking all present experimental studies into account, we have shown the anion and concentration dependent LCST values in Fig. 11. At all studied concentrations, the LCST values linearly decrease with increasing concentration of IL. However, the extent of decrease in LCST varies from IL to another IL depending upon their water structure making and breaking tendency. Indeed, the salting-out of an ion can be directly related to its Gibbs free energy of hydration ( $\Delta G_{\text{hyd}}$ ). Considering the fact that all ILs share a common imidazolium cation with different anions, it is easy to see that the anion with a higher salting-out ability has a more negative  $\Delta G_{\text{hyd}}$  values<sup>52</sup>:  $\text{CH}_3\text{COO}^-$ ,  $-365 \text{ kJ mol}^{-1}$  >  $\text{Cl}^-$ ,  $-340 \text{ kJ mol}^{-1}$  >  $\text{BF}_4^-$ ,  $-190 \text{ kJ mol}^{-1}$ . Thus, the Kosmotropic anions with more negative  $\Delta G_{\text{hyd}}$  value are stronger salting-out species, and therefore more prone to induce dehydration of polymer in aqueous media than that of chaotropic anion with less negative of  $\Delta G_{\text{hyd}}$  value. Hence, the hydration of chaotropic anions was not as strong as kosmotropic anions to induce dehydration of polymer in aqueous medium. Our results reveal that anion of IL has a great influence on the coil-globule transition state of aqueous PNIPAM solution. On the basis of tendency for lowering the LCST, the current studied anions of ILs have been arranged in the following order:  $\text{SCN}^- < \text{BF}_4^- < \text{I}^- < \text{Br}^- < \text{Cl}^- < \text{CH}_3\text{COO}^- < \text{HSO}_4^-$ .

Clearly, the extent of diminishment in LCST is more pronounced in the case of  $\text{HSO}_4^-$ , whereas, the diminishment in LCST is less pronounced in the case of  $\text{SCN}^-$ . Our systematic results clearly show that kosmotropic anion ( $\text{HSO}_4^-$ ) strongly binds to water molecules that causes a significant shift in the LCST of PNIPAM aqueous system at all investigated concentrations of IL, while chaotropic anions ( $\text{SCN}^-$  and  $\text{I}^-$ ) binds to water molecules weakly which have a little influence on the phase transition of PNIPAM aqueous system. This discrepancy mainly due to the small and/or polyvalent ions which are generally considered as “structure makers” or “positively hydrated”. In their presence, the normal water structure is rearranged in the electric field of the ion which leads to a state where the thermal motion of water in the neighbourhood of the ion is restricted as compared to the bulk water. Moreover, because of their small size and large charge, these ions are capable of polarising the water molecules which are bounded to amide group of polymer.

On the other hand, large and/or monovalent ions in comparison are “structure breakers” (or “negatively hydrated”). Around such ions, the water structure is less organized than bulk and the mobility of the concerned water molecules is also increased. Further, in spite of large size and small charge of these anions, they are capable to form direct bonding with PNIPAM molecules and thereby reduce the availability of binding sites to water molecules.<sup>12,53-55</sup> In addition to this, numerous investigations<sup>56-58</sup> have used the viscosity B coefficient to explore the ion-solvent interactions and thereby, calculated ordering and disordering tendency of ions on the solvent structure including water.

The solubility of PNIPAM in water is controlled by inter and intra molecular hydrogen bonds. These bonds are known to be greatly influenced by various additives. In this context, a great research work has been exploited on PNIPAM aqueous solution, particularly by using ionic salts as additives. It is especially noteworthy to compare the present experimental results of ILs in the PNIPAM aqueous solution with those of ionic salts in the PNIPAM aqueous solution. As it was revealed by Cremer et al.,<sup>12,60</sup> PNIPAM exhibits two step phase transition in the presence of sufficient concentration of kosmotropic anions ( $\text{CO}_3^{2-}$ ,  $\text{SO}_4^{2-}$ ,  $\text{H}_2\text{PO}_4^-$ ,  $\text{F}^-$ ). However, interestingly, in the present study we have observed single phase transition of PNIPAM in the presence of a series of ILs having different anions (including kosmotropes and chaotropes) with same cation,  $\text{Bmim}^+$ .

To check single phase transition of PNIPAM aqueous solution we have further performed temperature dependent fluorescence spectroscopy measurements for PNIPAM aqueous solution in the presence of ILs having  $\text{Cl}^-$ ,  $\text{CH}_3\text{COO}^-$  and  $\text{HSO}_4^-$  as anions with  $\text{Bmim}^+$  as cation at the concentration of 70 mg/mL (Fig. S16). However, we have not observed two phase transition even at this higher concentration of ILs. This is mainly because of the amide and hydrophobic portion of polymer undergo dehydration process simultaneously, i.e. at the same time and contributing to the single phase transition even in the sufficiently high concentration of kosmotropic and chaotropic anions of IL.

The hypothesized driving force behind the single phase transition of PNIPAM in the present study is that ion-ion pair interactions within the ILs. On the other hand, electrostatic interactions are present in the ionic salts. Obviously, the electrostatic interactions are stronger than the ion-ion pair interactions. Anion of IL can easily decouple from its cation, and thereby produce enough number of anions at single instance as temperature raises. Due to the large and enough number of anions, PNIPAM undergoes single step phase transition in the presence of series of ILs having different anions with same cation of IL. Further, in IL the

size of the cation is much larger than the anion size. Because of this large difference in size, anion can easily decouple from the cation. On the other hand, since the electrostatic interactions are present between ions of ionic salts, it is not as easy as in the case of IL, to decouple the anion from its cation in the ionic salts and thereby enough number of anions may not produce to dehydrate the PNIPAM.

The aforesaid assumptions can be explained perfectly by applying the “Fajans rule”<sup>60</sup> which was developed by Fajans in the year of 1923. According to Fajans rule a small, highly charged cations pull the electron cloud of anion, thereby developing the covalent character in ionic bonds of ionic salts. Polarization of a large anion by a small cation resulting in generation of covalent character in ionic salt is a very frequent phenomenon. However, this type of polarization in IL with large cation and small anion is very rare. Moreover, practically it seems hard because a soft cation holds its electron, while a hard anion cannot repel its electron cloud to become a nucleus. Further, in another instance in support of our hypothesis, number of studies purportedly reveal that the binding energy ( $\Delta E$ ) of the ion pairs in IL is smaller than that of ionic salts.<sup>61</sup> Moreover, in ILs hydrogen bond plays a crucial role in deciding the physical and chemical properties, whereas, electrostatic forces play a main role in ionic salts.<sup>61</sup>

### Conclusions

A series of ILs having different anions ( $\text{SCN}^-$ ,  $\text{BF}_4^-$ ,  $\text{I}^-$ ,  $\text{Br}^-$ ,  $\text{Cl}^-$ ,  $\text{CH}_3\text{COO}^-$  and  $\text{HSO}_4^-$ ) with same cation ( $\text{Bmim}^+$ ) were employed to explore the influence of ILs on LCST behaviour of PNIPAM aqueous solution. These anions induce self-assembly of PNIPAM into nano-scale range particles in aqueous solution and decrease the LCST of PNIPAM. However, the extent of diminishment in LCST is more pronounced in the case of kosmotropes than that of chaotropes at all studied concentrations. In stark contrast to the previous reports, in the present experimental studies we have observed single phase transition even in the sufficient amount of IL. Ion specific interactions with hydration layer of PNIPAM in aqueous solution were further compared with the corresponding interactions with BSA molecules. Our results conclude that the affinity of the anions for water molecules depends on its chemical environment. Our results taken together with Cremer’s group results clearly show that structural changes (cation size and its nature) are macroscopically manifested through changes in the chemical environment and thereby the additives in polymer aqueous solution play an important role in obtaining the phase transition. The striking results, however, markedly depending on the type of additive added, type of interactions between ions in IL,



and nature of cation of IL too. However, further investigations are required to explore the effect of ILs having different cations and same anion on thermoresponsive polymers as an additive. These are currently under progress in our laboratory. Finally, we have validated our experimental results by applying the same series of ILs of different anions with same cation on BSA.

### **Acknowledgements**

We acknowledge the financial support from the Department of Science and Technology (DST), New Delhi, India (Grant No. SB/SI/PC-109/2012). We are highly thankful to the Mr. Amit, Malvern, Aimil Ltd., New Delhi, Dr. Ruchitha Pal, Advanced Instrumentation Facility Centre of Jawaharlal Nehru University, New Delhi and Mr. Aniruddha Pisal, Thermo Fisher Scientific, Mumbai, India for providing DLS, SEM and FTIR facilities, respectively.

## References

1. J. Hao, G. Yuan, W. He, H. Cheng, C. C. Han and C. Wu, *Macromolecules*, 2010, **43**, 2002–2008.
2. Y. Lu, K. Zhou, Y. Ding, G. Zhang and C. Wu, *Phys. Chem. Chem. Phys.*, 2010, **12**, 3188–3194.
3. P. Venkatesu, *J. Phys. Chem. B*, 2006, **110**, 17339–17346.
4. R. Barbey, L. Lavanant, D. Paripovic, N. Schuwer, C. Sugnaux, S. Tugulu and H. A. Klok, *Chem. Rev.*, 2009, **109**, 5437–5527.
5. P. M. Mendes, *Chem. Soc. Rev.*, 2008, **37**, 2512–2529.
6. S. Amemori, K. Kokado and K. Sada, *J. Am. Chem. Soc.*, 2012, **134**, 8344–8347.
7. P. M. Reddy and P. Venkatesu, *J. Phys. Chem. B*, 2011, **115**, 4752–4757.
8. P. M. Reddy, M. Taha, P. Venkatesu, A. Kumar, and M. J. Lee, *J. Chem. Phys.*, 2012, **136**, 234904-234910.
9. F. Tanaka, T. Koga and F. M. Winnik, *Phys. Rev. Lett.*, 2008, **101**, 028302-028304.
10. C. Morris, B. Szczupak, A. S. Klymchenko and A. G. Ryder, *Macromolecules*, 2010, **43**, 9488–9494.
11. N. Al-Manasir, K. Zhu, A. L. Kjøniksen, K. D Knudsen, G. Karlsson and B. Nystrom, *J. Phys. Chem. B*, 2009, **113**, 11115–11123.
12. Y. Zhang, S. Furyk, D. E. Bergbreiter and P.S. Cremer, *J. Am. Chem. Soc.*, 2005, **127**, 14505–14510.
13. F. Meersman, J. Wang, Y. Wu and K. Heremans, *Macromolecules*, 2005, **38**, 8923–8928.
14. P. M. Lopez-Perez, R. M. P. Da Silva, I. Pashkuleva, F. Parra, R. L. Reis and J. S. Roman, *Langmuir*, 2010, **26**, 5934–5941.
15. E. I. Tiktopulo, V. N. Uversky, V. B Lushchik, S. I. Klenin, V. E Bychkova and O. B. Ptitsyn, *Macromolecules*, 1995, **28**, 7519–7524.
16. D. Dhara and P. R. Chatterji, *J. Macromol. Sci.*, 2000, **40**, 51–68.
17. A. Zhuk, R. Mirza and Sukhishvili, *ACS Nano.*, 2011, **5**, 8790–8799.
18. R. Freitag and F. Garret-Flaudy, *Langmuir*, 2002, **18**, 3434–3440.
19. Y. Zhang, S. Furyk, L. B. Sagle, Y. Cho, D. E. Bergbreiter and P. S. Cremer, *J. Phys. Chem. C*, 2007, **111**, 8916–8924.
20. L. T. Lee and B. Cabane, *Macromolecules*, 1997, **30**, 6559-6566.
21. P. W. Zhu and D. H. Napper, *Langmuir*, 1996, **12**, 5992–5998.

22. R. Walter, J. Ricka, C. H. Quellet, R. Nuffenger and T. H. Binkert, *Macromolecules* 1996, **29**, 4019–4028.
23. F. M. Winnik, M. F. Ottaviani, S. H. Bossmann, M. Garcia-Garibay and N. J. Turro, *Macromolecules*, 1992, **25**, 6007–6017.
24. F. Tanaka, T. Koga, H. Kojima and F. M. Winnik, *Macromolecules*, 2006, **42**, 1321–1330.
25. J. Pang, H. Yang, J. Ma and R. Cheng, *J. Phys. Chem. B*, 2010, **114**, 8652–8658.
26. B. L. Sagle, Y. Zhang, V. A. Litosh, X. Chen, Y. Cho and P. S. Cremer, *J. Am. Chem. Soc.*, 2009, **131**, 9304–9310.
27. A. Shpigelman, Y. Paz, O. Ramon and Y. D. Livney, *Colloid. Polym. Sci.*, 2011, **289**, 281–290.
28. H. Du, R. Wickramasinghe and X. Qian, *J. Phys. Chem. B*, 2010, **114**, 16594–16604.
29. E. A. Algaer, and N. F. A. van der Vegt, *J. Phys. Chem. B*, 2011, **115**, 13781–13787.
30. K. B. Rembert, J. Paterová, J. Heyda, C. Hilty, P. Jungwirth and P. S. Cremer, *J. Am. Chem. Soc.*, 2012, **134**, 10039–10046.
31. T. Ueki, Y. Nakamura, A. Yamaguchi, K. Niitsuma, T. P. Lodge and M. Watanabe, *Macromolecules*, 2011, **44**, 6908–6914.
32. T. Ueki, Y. Nakamura, T. P. Lodge and M. Watanabe, *Macromolecules*, 2012, **45**, 7566–7573.
33. A. Kumar and P. Venkatesu, *Chem. Rev.*, 2012, **112**, 4283–4307.
34. P. Attri, P. M. Reddy, P. Venkatesu, A. Kumar and T. Hofman, *J. Phys. Chem. B*, **114**, 6126–6133.
35. C. Lange, G. Patil and R. Rudolph, *Protein. Sci.*, 2005, **14**, 2693–2701.
36. C. A. Summers, and R. A. Flowers, *Protein. Sci.*, 2010, **9**, 2001–2008.
37. P. Attri and P. Venkatesu, *Int. J. Biol. Macromol.*, 2012, **51**, 119–128.
38. A. Kumar, P. M. Reddy and P. Venkatesu, *RSC Advances*, 2012, **2**, 6939–6947.
39. A. Kumar, P. M. Reddy and P. Venkatesu, *New. J. Chem.*, 2012, **36**, 2266–2279.
40. R. G. Reed, *J. Biol. Chem.*, 1997, **252**, 7483–7487.
41. A. Beyaz, S. O. Woon and V. P. Reddy, *Colloids Surf. B*, 2004, **35**, 119–124.
42. L. Stryer, *J. Mol. Biol.*, 1965, **13**, 482–495.
43. P. B. S. Junior, V. A. O. Tiera and M. Tiera, *J. Ecl. Quím. São. Paulo.*, 2007, **32**, 47–54.
44. O. Zheng and J. X. Zhao, *J. Colloid Interface Sci.*, 2006, **300**, 749–754.

45. G. Staikos, *Macromol. Rapid. Commun.*, 1995, **16**, 913-917.
46. M. Tsianou, A. L. Kjoniksen, K. Thuresson and B. Nystrom, *Macromolecules*, 1999, **32**, 2974-2982.
47. M. Taha, B. S. Gupta, I. Khoiroh and M. J. Lee, *Macromolecules*, 2011, **44**, 8575-8589.
48. H. Yamauchi and Y. Maeda, *J. Phys. Chem. B*, 2007, **111**, 12964-12968.
49. Y. Maeda, T. Higuchi, and I. Ikeda, *Langmuir*, 2000, **16**, 7503-7509.
50. A. C. Kumar, H. B. Bohidar and A. K. Mishra, *Colloids Surf. B*, 2009, **70**, 60-67.
51. A. C. Kumar, H. Erothu, H. B. Bohidar and A. K. Mishra, *J. Phys. Chem. B*, 2011, **115**, 433-439.
52. Y. Marcus, *J. Chem. Soc. Farad. Trans.*, 1991, **87**, 2995-2999.
53. E. Florin, R. Kjellander and J. Eriksson, *J. Chem. Soc. Faraday Trans.*, 1985, **80**, 2889-2910.
54. O. Samoilov, *Wiley-Interscience, New York*, 1972.
55. H. S. Frank and W. Y. Wen, *Discuss Faraday Soc.*, 1957, **24**, 133-140.
56. G. Jones and M. Dole, *J. Am. Chem. Soc.*, 1929, **51**, 2950-2964.
57. M. Salomäki, P. Tervasmäki, S. Areva and J. Kankare, *Langmuir*, 2004, **20**, 3679-3683.
58. H. D. B. Jenkins and Y. Marcus, *Chem. Rev.*, 1965, **95**, 2695-2724.
59. Y. Zhang and P. S. Cremer, *Annu. Rev. Phys. Chem.*, 2010, **61**, 63-83.
60. K. Fajans, *Naturewiss*, 1923, **11**, 165-172.
61. K. Dong and S. Zhang, *Chem. Eur. J.*, 2012, **18**, 2748-2761.

## Figure Captions

**Fig.1** Chemical structure of PNIPAM.

**Fig. 2** UV-visible absorbance spectra of ANS in PNIPAM aqueous solution without and with ILs; {IL free (black colour line),  $\text{SCN}^-$  (green colour line),  $\text{BF}_4^-$  (blue colour line),  $\text{I}^-$  (dark yellow colour line),  $\text{Br}^-$  (cyan colour line),  $\text{Cl}^-$  (magenta colour line),  $\text{CH}_3\text{COO}^-$  (red colour line) and  $\text{HSO}_4^-$  (yellow colour line)} at 25 °C. Concentration IL is 5 mg/mL.

**Fig. 3** Fluorescence emission spectra of ANS in PNIPAM aqueous solution without and with ILs; {pure ANS (navy blue line), IL free (black colour line),  $\text{SCN}^-$  (green colour line),  $\text{BF}_4^-$  (blue colour line),  $\text{I}^-$  (dark yellow colour line),  $\text{Br}^-$  (cyan colour line),  $\text{Cl}^-$  (magenta colour line),  $\text{CH}_3\text{COO}^-$  (red colour line) and  $\text{HSO}_4^-$  (yellow colour line)} at 25 °C. Concentration of IL is 5 mg/mL.

**Fig. 4** Temperature dependent fluorescence emission spectra of ANS in PNIPAM aqueous solution without and with ILs; {IL free (black colour line),  $\text{SCN}^-$  (green colour line),  $\text{BF}_4^-$  (blue colour line),  $\text{I}^-$  (dark yellow colour line),  $\text{Br}^-$  (cyan colour line),  $\text{Cl}^-$  (magenta colour line),  $\text{CH}_3\text{COO}^-$  (red colour line) and  $\text{HSO}_4^-$  (yellow colour line)} in the temperature range of 25 – 40 °C. Concentration of IL is 5 mg/mL.

**Fig. 5** Viscosity of the PNIPAM aqueous solution without and with ILs; {IL free (black colour line),  $\text{SCN}^-$  (green colour line),  $\text{BF}_4^-$  (blue colour line),  $\text{I}^-$  (dark yellow colour line),  $\text{Br}^-$  (cyan colour line),  $\text{Cl}^-$  (magenta colour line),  $\text{CH}_3\text{COO}^-$  (red colour line) and  $\text{HSO}_4^-$  (yellow colour line)} in the temperature range of 25 – 40 °C. Concentration of IL is 5 mg/mL.

**Fig. 6** Hydrodynamic diameter,  $d_H$ , of PNIPAM in the absence and presence of ILs; {IL free (black colour line),  $\text{SCN}^-$  (green colour line),  $\text{BF}_4^-$  (blue colour line),  $\text{I}^-$  (dark yellow colour line),  $\text{Br}^-$  (cyan colour line),  $\text{Cl}^-$  (magenta colour line),  $\text{CH}_3\text{COO}^-$  (red colour line) and  $\text{HSO}_4^-$  (yellow colour line)} in the temperature range of 25 – 40 °C. Concentration of IL is 5 mg/mL.

**Fig. 7** FTIR spectra spectra of PNIPAM aqueous solution without and with ILs; {IL free (black colour line),  $\text{SCN}^-$  (green colour line),  $\text{BF}_4^-$  (blue colour line),  $\text{I}^-$  (dark yellow colour line),  $\text{Br}^-$  (cyan colour line),  $\text{Cl}^-$  (magenta colour line),  $\text{CH}_3\text{COO}^-$  (red colour line) and  $\text{HSO}_4^-$  (yellow colour line)} at 25 °C. Concentration IL is 5 mg/mL.

**Fig. 8** SEM micrographs of an aqueous solution of PNIPAM without ionic liquid (a), with IL containing  $\text{SCN}^-$  anion (b) and  $\text{HSO}_4^-$  anion (c) of concentration of 10 mg/mL and  $\text{SCN}^-$  anion (d) and  $\text{HSO}_4^-$  anion (e) of concentration of 15 mg/mL.

**Fig. 9** The influence of [Bmim][ $\text{HSO}_4$ ] IL, 0 mg/mL (black colour line), 5 mg/mL (red colour line), 10 mg/mL (green colour line) and 15 mg/mL (blue colour line) on PNIPAM aqueous solution. (a) UV-visible absorbance spectra, (b) fluorescence emission spectra, (c) temperature dependent fluorescence emission spectra, (d) viscosity measurements, (e) DLS measurements and (f) FTIR spectra analysis. However, for the sake of clarity presentation, we have not provided other IL concentrations effect on PNIPAM aqueous solution, since we observed the similar trend for other ILs.

**Fig. 10** UV-visible absorbance spectra of tryptophan of BSA in the aqueous solution without and with ILs; {IL free (black colour line),  $\text{SCN}^-$  (green colour line),  $\text{BF}_4^-$  (blue colour line),  $\text{I}^-$  (dark yellow colour line),  $\text{Br}^-$  (cyan colour line),  $\text{Cl}^-$  (magenta colour line),  $\text{CH}_3\text{COO}^-$  (red line colour) and  $\text{HSO}_4^-$  (yellow colour line)} at 25 °C. Concentration of IL is 5 mg/mL.

**Fig. 11** LCST values of PNIPAM aqueous solution as a function of anion and concentration of IL; { $\text{SCN}^-$  (green colour line),  $\text{BF}_4^-$  (blue colour line),  $\text{I}^-$  (dark yellow colour line),  $\text{Br}^-$  (cyan colour line),  $\text{Cl}^-$  (magenta colour line),  $\text{CH}_3\text{COO}^-$  (red colour line) and  $\text{HSO}_4^-$  (yellow colour line)}.

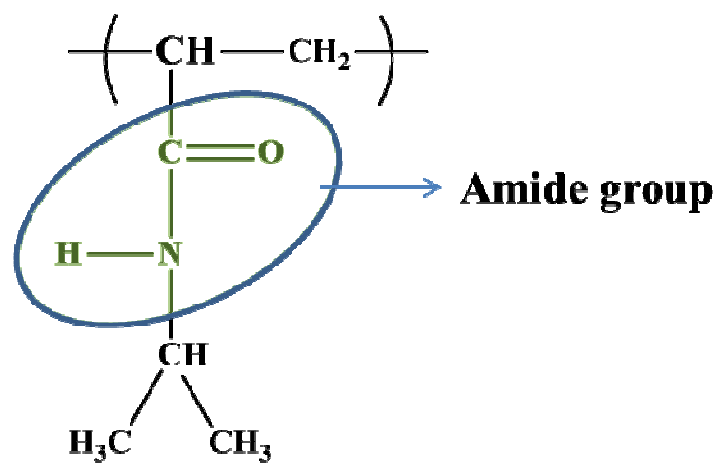


Fig. 1

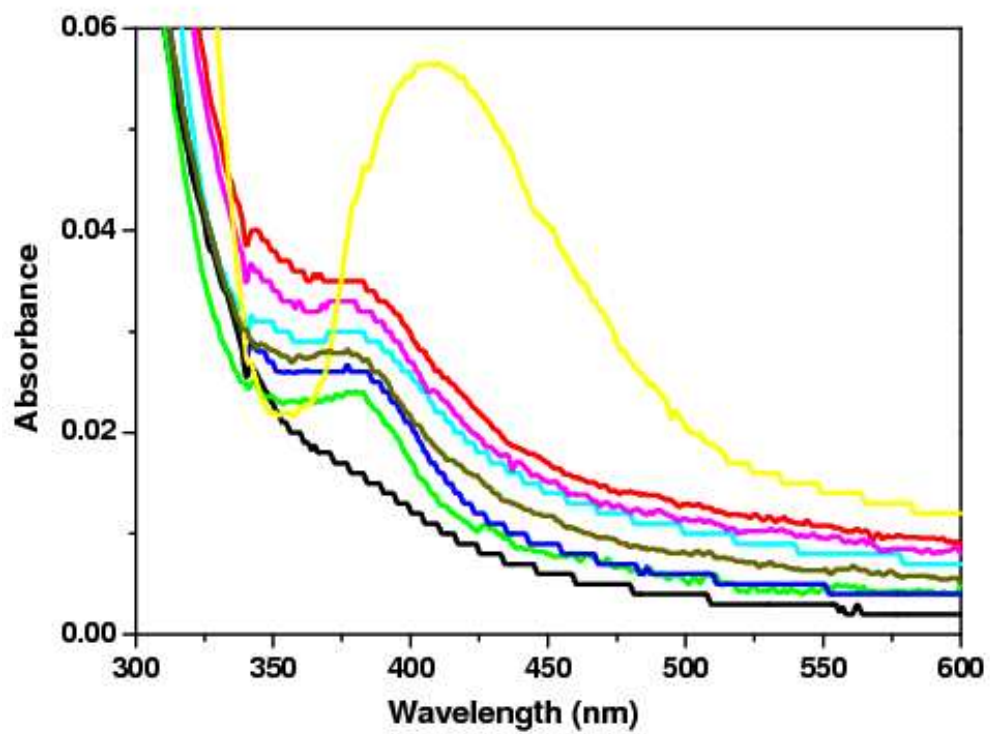


Fig. 2



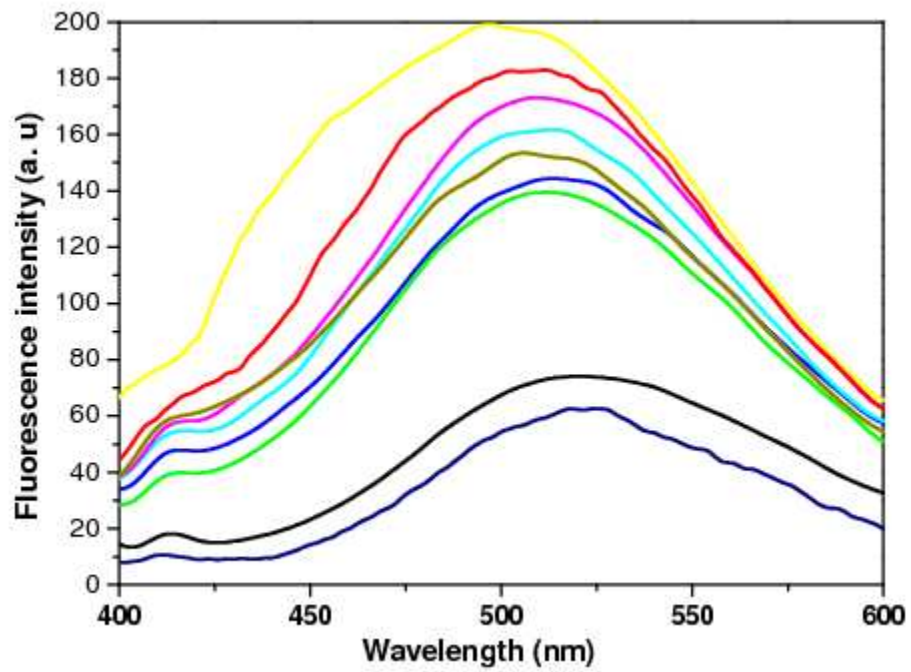


Fig. 3

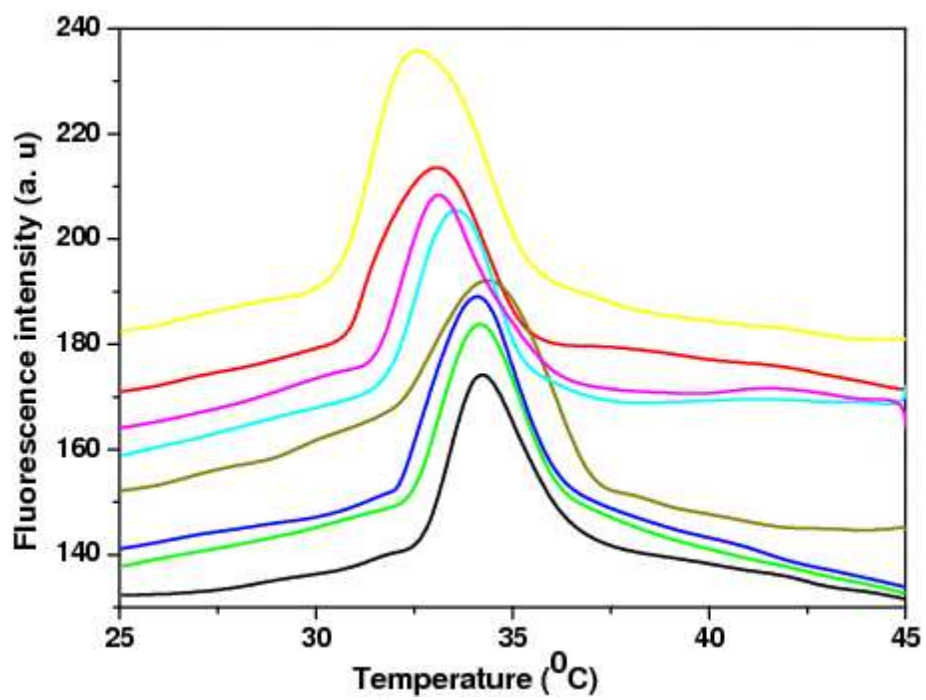


Fig. 4

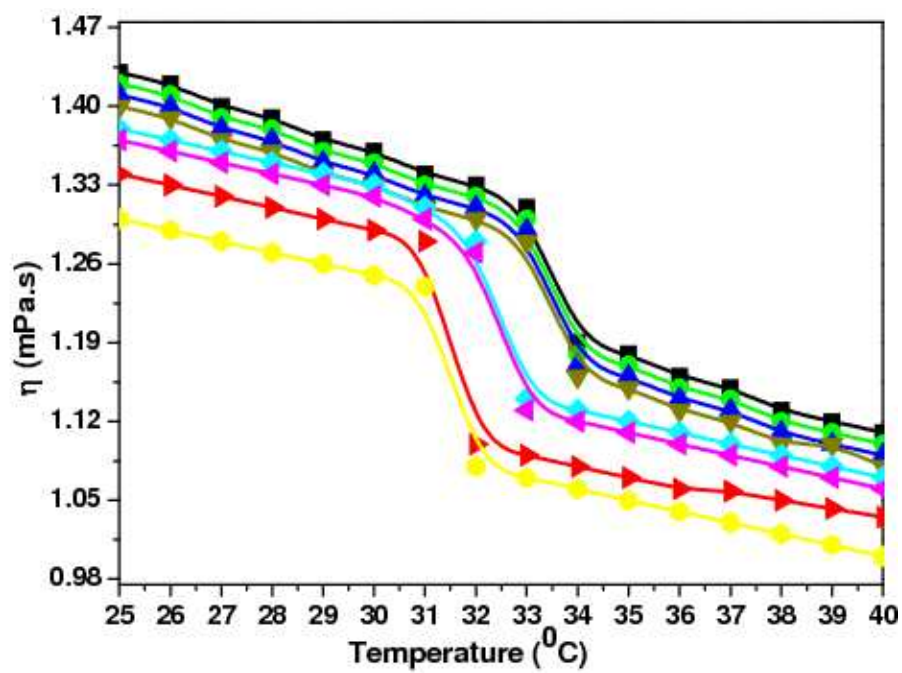


Fig. 5

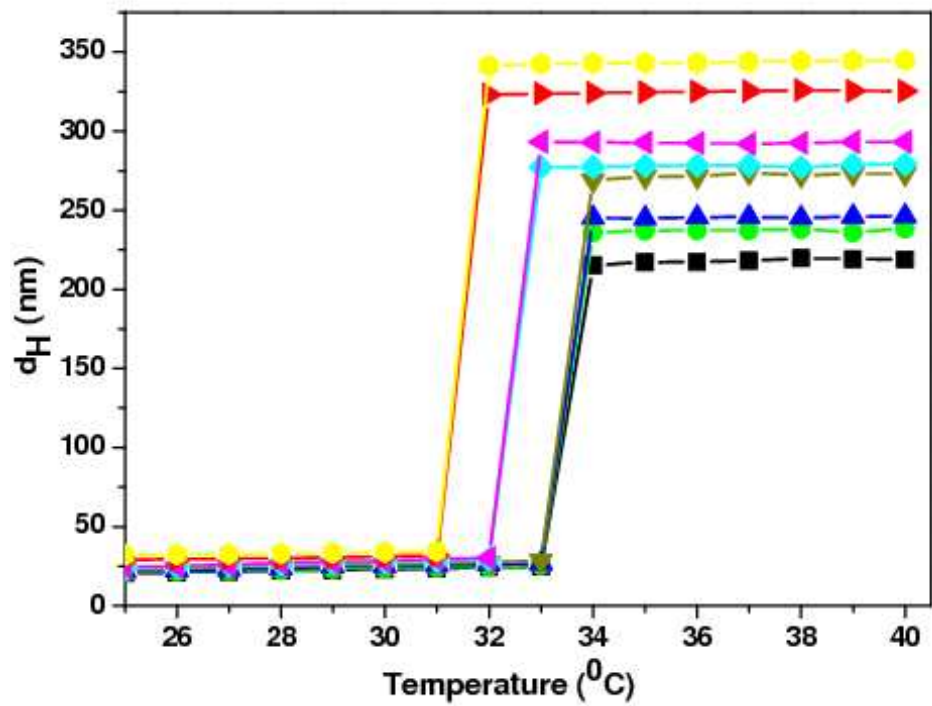


Fig. 6

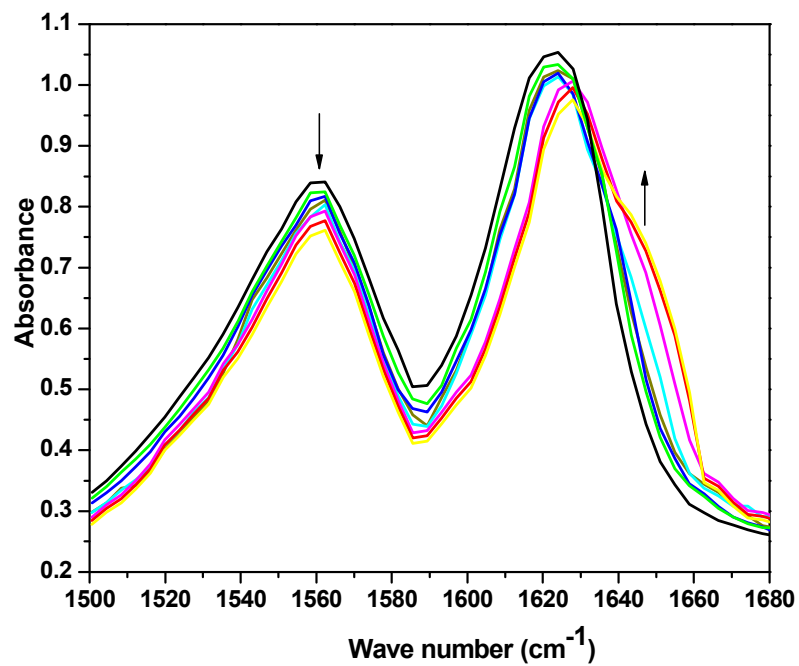


Fig. 7

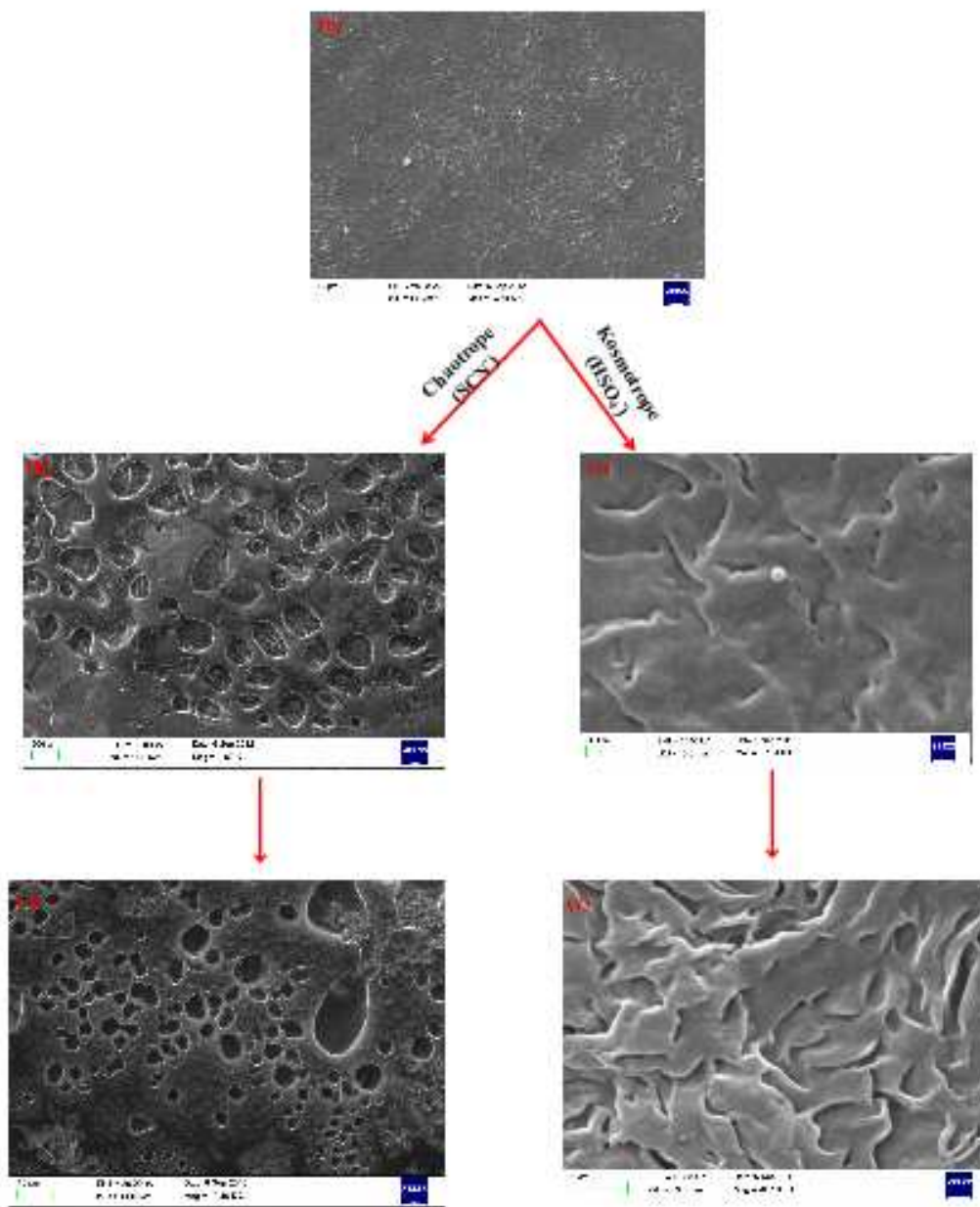


Fig. 8

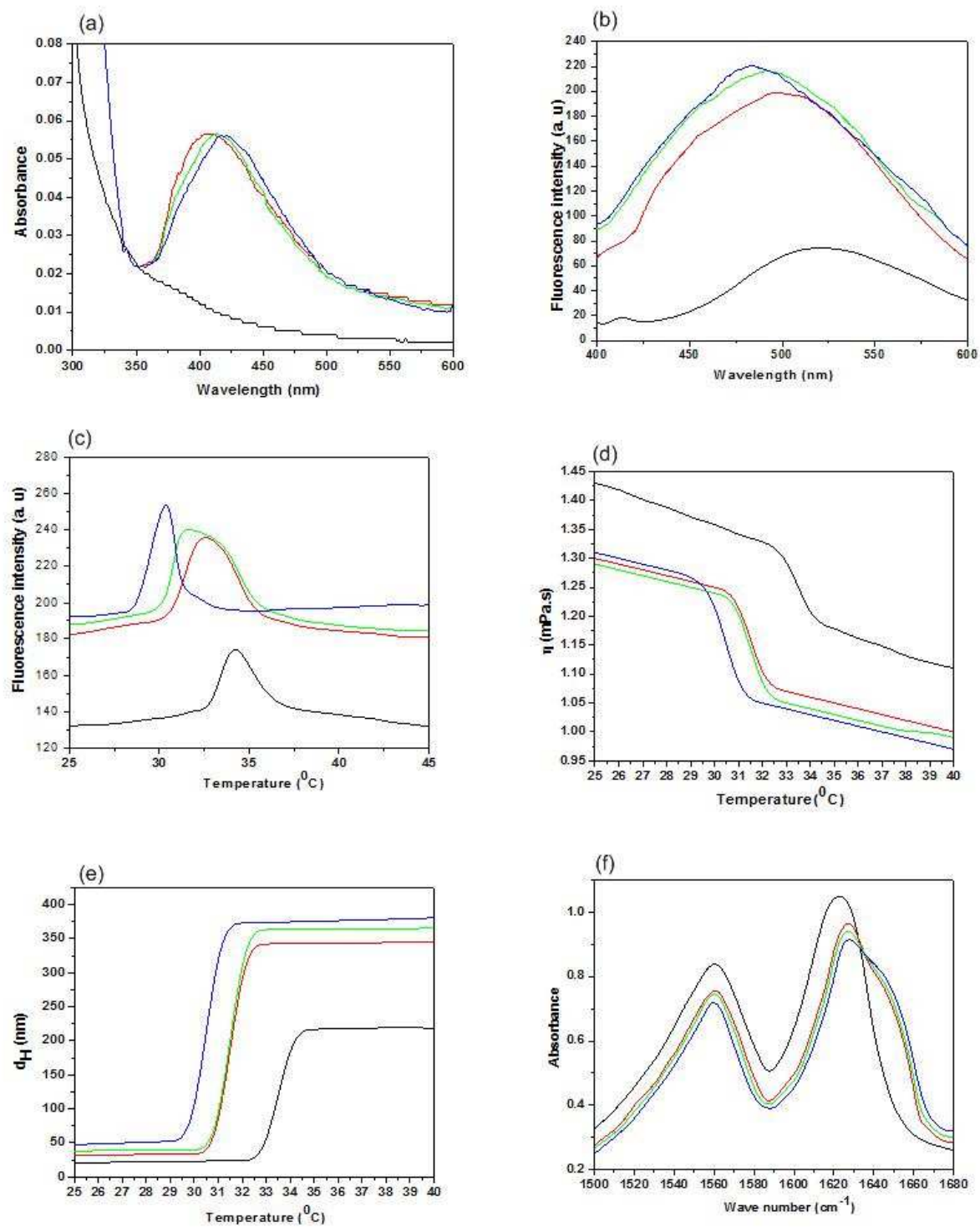


Fig. 9

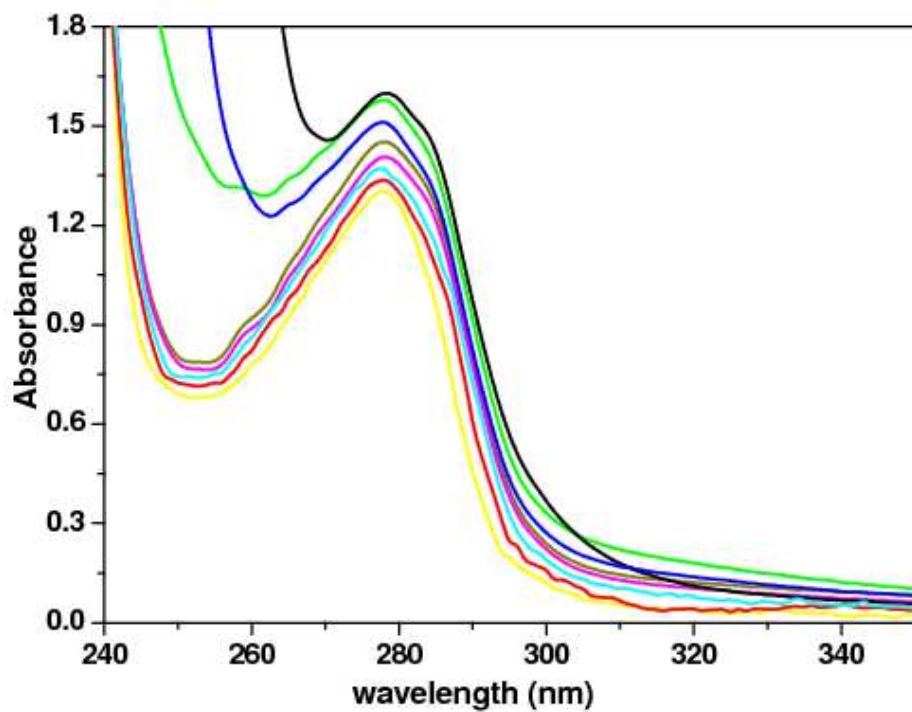


Fig. 10



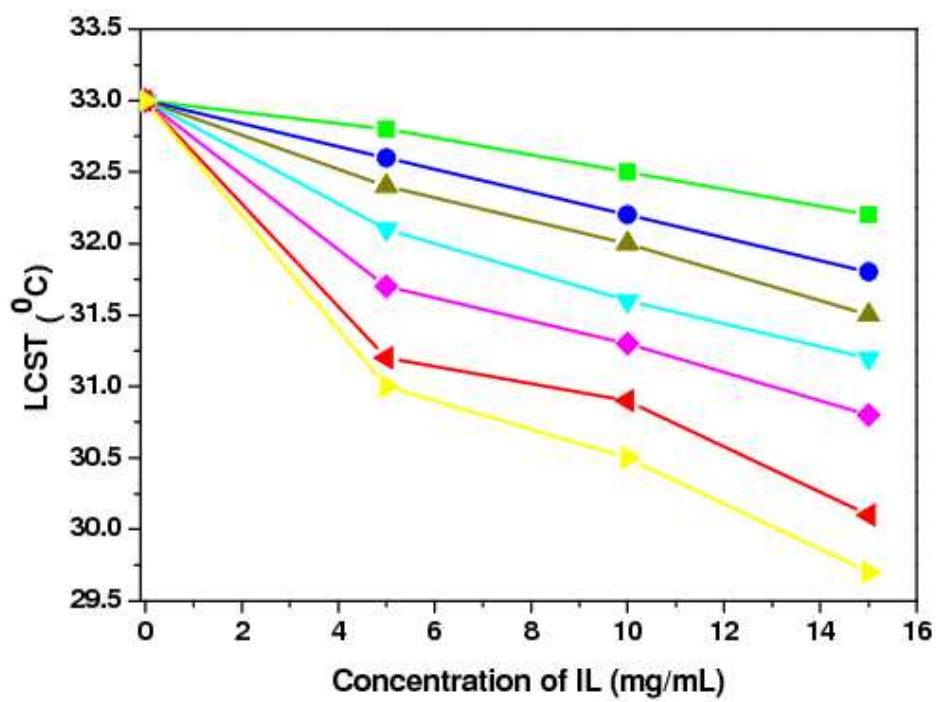


Fig. 11